

Novel Proton Exchange Membranes Based on Sulfonated Cellulose Acetate for Fuel Cell Applications: Preparation and Characterization

M. S. Mohy Eldin^{1,2,*}, M. H. Abd Elmageed³, A. M. Omer², T. M. Tamer², M. E. Yossuf⁴, R. E. Khalifa²

¹ Chemistry Department, Faculty of Science, University of Jeddah, Asfan, P. O. Box: 80203, Jeddah 21589, Saudi Arabia

² Polymer Materials Research Department, Advanced Technology and New Materials Research Institute, MuCSAT, New Borg El-Arab City 21934, Alexandria, Egypt

³ Chemical Engineering Department, Faculty of Engineering, Alexandria University, Alexandria, Egypt.

⁴ Computer-Based Engineering Applications Department, Informatics Research Institute, MuCSAT, New Borg El-Arab City 21934, Alexandria, Egypt

* E-mail: m.mohyeldin@mucsat.sci.eg

Received: 6 February 2016 / *Accepted:* 16 April 2016 / *Published:* 10 November 2016

A novel sulfonated cellulose acetate (SCA) membranes synthesized for the first time as a proton exchange membrane for direct membrane fuel cells (DMFCs). Cellulose acetate was activated using epichlorohydrin (ECH) followed by doping the activated membranes in sodium sulfite solution later on. The chemical structure and surface properties of SCA membranes confirmed by Infrared spectrophotometric analysis (FTIR). Morphological characterization was examined using scanning electron microscopy (SEM). The thermal stability of the prepared membranes tested by the thermogravimetric analysis (TGA). Results indicated that SCA membranes were thermally stable up to 375.72°C. Interestingly, investigating essential characters required for polyelectrolyte membrane for fuel cell application show that the ion exchange capacity (IEC) estimated in the range of 0.369–0.996 meq/g compared to 0.9 meq/g for Nafion[®]117. Furthermore, long membrane lifetime under oxidative conditions (Fenton's reagent), high mechanical properties (49.25N), good dimensional stability, low water and methanol uptake. In addition to, lower methanol permeability (1.729×10^{-17} cm²/S) compared to (1.14×10^{-9} cm²/S) for Nafion[®]117. These results make the low-cost SCA membranes a promising polyelectrolyte for direct methanol fuel cell application.

Keywords: Cellulose acetate; Proton exchange membrane; Direct methanol fuel cell; Ion exchange capacity; Methanol permeability.

1. INTRODUCTION

During the last decades, DMFCs which use liquid methanol directly as a fuel feed to convert the chemical energy efficiently into electrical energy have received significant attention as a promising alternative clean power generators [1-3]. Owing to their simple design, stable operation at relatively low temperature, high efficiency, the high power density at high methanol concentration, low noise, less weight, easy production, storage and transportation of liquid methanol [4-6]. Besides, DMFCs suppress global warming [7] as it save fossil fuels and cause little environmental pollution [8] especially carbon dioxide emissions. The development of DMFCs has been paid much interest particularly for fuel cell applications in transportation, distributed power, and future portable sources of energy. Polymer electrolyte membranes (PEMs) which considered the heart of the fuel cell are one of the key components of DMFCs [9-10] because it mediates ionic pathways to transfer protons from the anode to the cathode site. Furthermore acting as a barrier between the reactant gas and prevent direct combustion. To achieve high fuel cell efficiencies PEMs must simultaneously possess the following properties to be successfully commercialized such as; negligible electronic conductivity, low costs, availability, excellent chemical and thermal stability, increased durability under the operating conditions, adequate mechanical and electrochemical stability. Moreover, PEMs are evaluating firstly by two main fundamental properties namely the proton conductivity and the methanol permeability. However, the industrialization of DMFCs is hindered by two major drawbacks affecting the overall cell performance. Firstly, the undesirable transport of methanol from the anode to the cathode through PEM called methanol crossover phenomenon [11] which results in significant problems such as 20% of parasitic fuel loss and lower cell voltage when Nafion[®] membranes used [12], poisoning of the catalyst and unacceptable reduction in fuel efficiency. Secondly, slow kinetics of the oxidation reaction of methanol at the anode. Up to now, perfluoro sulfonic acid membranes such as Nafion[®] manufactured by DuPont, with fluoroalkyl ether side chains and sulfonic acid end groups, are the most widespread PEM membranes for fuel cell applications. Due to their high proton conductivity in humidified conditions and at intermediate temperatures below 80°C as it degrades at higher temperatures than 110–130°C [13], high permeability to protons [14], extremely high oxidative stability, excellent chemical stability, and reasonable mechanical properties. The great successes with Nafion[®] membranes in hydrogen fuel cells do not guaranty the commercialization in DMFCs applications. The objects can summarize as the high cost, complicated processing, limitation in operation temperature, the decrease in proton conductivity at high temperature, thermal instability which causes physical shrinkage of Nafion[®] membranes, and slow anode kinetics and high methanol permeability. Therefore, Many efforts, has been focused on developing new proton conductive membranes to overcome these obstacles through two main stratagems. One of them through the modification of perfluoro sulfonic acid membranes such as blending Nafion[®] with other polymers, synthesis of Nafion[®] composites with inorganic nanoparticles or blocking Nafion surface by metallic layers [15]. The other is to replace Nafion[®] membranes with cheaper, eco-friendly and more acceptable non-fluorinated materials as PEMs for DMFCs. Presently, various academic and industrial groups are focusing on developing families of polymers with different chemical structures and functionalized with sulfonic acid groups because of their low cost, high proton conductivity, excellent

thermal, chemical and mechanical stabilities [16-18]. Among these proposed alternative polymer-sulfonated poly (ether ether ketone) (SPEEK) [19,20] , sulfonated polysulfone (SPSf) [21] , and sulfonated polyimide (SPI) [22-24] , sulfonated poly(aryl ether sulfone)s (SPAES) [25] , poly(phenyl sulfide sulfone)s (PPSS) [26] , sulfonated Polybenzimidazoles (PBI) [27,28] , poly(styrene sulfonic acid) (PSS) [29], sulfonated poly (phthalazinone ether nitrile ketone) (PPENK) [30], and sulfonated poly(ether ketone) (SPEK) [31-33], and poly(arylene ether) (PAE) copolymers containing aromatic nitriles [34] , poly(ether sulfone) (PES) [35] and sulfonated poly(arylene ether ketone)s (SPAEK) [36] . Usually, the introducing of sulfonic acid groups into the polymer backbone may be achieved either by direct sulfonation of the base polymers or by polymerization of sulfonated monomers with different sulfonation levels to achieve reflective properties of the prepared proton conducting membranes. In this study novel sulfonated proton exchange membranes for DMFCs applications based on a modified natural polymer such as cellulose acetate (CA) prepared and characterized. The synthesis of the membranes including the activation of CA structure using epichlorohydrin and consequently the activated membranes was doped with sodium sulfite solution to introduce sulfonic acid group. Factors affecting the activation and sulfonation processes were studied such as concentration, time, temperature and solvent ratios to explore the optimum conditions. SCA membranes characterized by FTIR, TGA, SEM and XRD analysis. The membranes performances extensively investigated regarding mechanical stability, water, and methanol uptake, dimensional stability and methanol permeability. The obtained results postulated that SCA membranes exhibit suitable properties for fuel cell applications as well as DMFCs.

2. EXPERIMENTAL

2.1. Materials

Cellulose acetate powder (Degree of acetylation 40%) and Epichlorohydrin (purity 99.5%) supplied by Sigma- Aldrich Chemie GmbH (USA). Acetone (purity 90%) and Sulfuric acid (purity 95-97%) were provided by Sigma-Aldrich (Germany). Methanol (purity 99.8%) provided from Fluka Chemie GmbH (Switzerland). Ethyl alcohol absolute, Sodium Sulfite, Sodium Hydroxide, Hydrogen Peroxide and Phenol phthalin purchased from El- Nasr Pharmaceutical Co for Chemicals (Egypt). Hydrochloric acid (purity 37%) obtained from Polska Odczynniki Chemiczne S.A. (Finland).

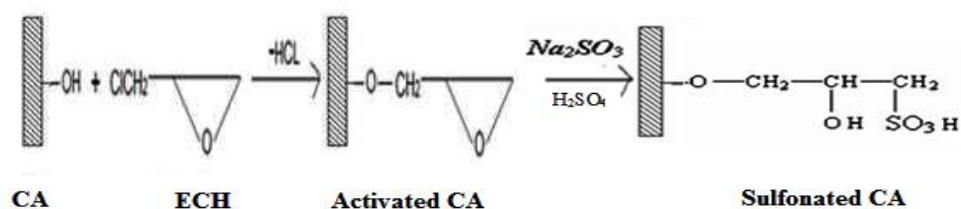
2.2. Methods

2.2.1. Membrane preparation

Sulfonation step

Cellulose acetate powder (CA) was epoxidated through the activation with ECH as described in our previous work [37]. Briefly, the synthesis of activated CA membranes was achieved by the addition of ECH to the aqueous solution of CA in molar ratio 1:3, CA: ECH respectively at 55°C for

12h. Then the solution was casting on a glass petri dish and allowed to dry in a vacuum oven for 12h. The obtained membranes were washed several times with methanol solution to remove the excess amount of ECH. The activated CA membranes with dimension (4cm × 5cm) dipped in 0.25-6% sodium sulfite which dissolved in 30% ethanol-water solution for 2h at 35°C (Scheme 2). The effect of solvent ratio studied by variation the ethanol content from 25% to 50% (V/V). The dipped membranes were then acidified using an excess amount of 2M H₂SO₄ aqueous solution for 2h under shaking at ambient temperature to exchange Na⁺ ions with H⁺ ions. Finally, the resultant sulfonated cellulose acetate (SCA) membranes were rinsed several times with distilled water to remove the free acid.



Scheme 1. The proposed mechanistic pathway for synthesis of sulfonated cellulose acetate.

2.2.2. Membrane characterization

Water and methanol uptake

Samples for water and methanol uptake were dried in vacuum for 24h at 40°C and then cut into 2cm². All samples weighed in the dry state before swelling in water or methanol. Then, soaked in water or/ methanol, which placed in a closed glass container at ambient temperature overnight. After that, the swollen membranes were removed, and the excess of water or methanol quickly wiped with tissue paper and weighed immediately. The liquid uptake (water or methanol) calculated by setting the weight difference between the dry and wet membranes using the following equation [38]:

$$LU(\%) = \frac{W_w - W_d}{W_d} \times 100 \quad (1)$$

Where W_d and W_w are the dry weight and the wet weight of the membrane samples, respectively.

Dimensional change

The dimension changes were carried out by immersing the prepared membranes into deionized water or pure methanol [39] at room temperature for 24h. The percentage of the changed area (ΔA %) calculated according to the following equation:

$$\Delta A\% = \frac{A - A_o}{A_o} \times 100 \quad (2)$$

Where A_0 and A is the area of the membrane before and after soaking treatment, respectively.

Infrared spectrophotometric analysis (FTIR)

Functional groups investigation in original, activated and sulfonated membranes having different concentration was carried out using Fourier transform infrared spectrophotometer (Shimadzu FTIR-8400 S), Japan.

Thermal gravimetric analysis (TGA)

Thermal characterization of all membranes having different concentration was carried out using thermogravimetric analyzers (Shimadzu TGA-50, Japan).

Scanning electron microscopic analysis (SEM)

Surface characterization of the original, activated and sulfonated membranes was carried out using energy-dispersive analysis X-ray (Joel 6360LA), Japan.

X-Ray diffraction analysis (XRD)

X-ray patterns of the native CA, activated CA and sulfonated CA membranes obtained using (Schimadzu7000) diffractometer.

Surface roughness

The surface roughness was determined using surface roughness tester (SJ- 201P), Japan. Samples mounted on a glass slide with a double-sided tab. Minimum sample dimensions were 4cm×5cm. All results are the average of six measurements.

Thermal oxidative stability

The oxidative stability evaluated by estimating the weight changes of the membranes in Fenton's reagent. Small pieces of membrane samples (2cm×2cm) were placed into Fenton's reagent (4ppm FeSO_4 in 3% H_2O_2) at 80°C under stirring. At regular intervals, the samples were removed from the solution and quickly weighed after removing the surface liquid with filter paper. The Fenton's

reagent refreshed every 10h [40].

Optical properties (Colorimeter)

The color change during the membranes surface was measured using a colorimeter. The film color detected by an X-Rite Model Sp64 Made in the USA. The colorimeter calibrated with white and black plates. A white standard color plate for the instrument calibration used as a background for color measurements of the films [37]. The system provided the values of three color components namely, L^* (black-white component, luminosity), and the Chromatics coordinates, a^* (+red to -green component) and b^* (+yellow to -blue component). Color differences ΔE^* were also calculated by the following equation:

$$\Delta E = \sqrt{(\Delta L^*)^2 + (\Delta a^*)^2 + (\Delta b^*)^2} \quad (3)$$

Where: $\Delta L^* = L^* - L_0^*$, $\Delta a^* = a^* - a_0^*$, $\Delta b^* = b^* - b_0^*$ being: L_0^* , a_0^* , b_0^* are the color parameter values of the standard and L^* ; a^* ; b^* the color parameter values of the sample.

2.2.3. Ion exchange capacity

The degree of sulfonation, which is the number of sulfonic acid groups ($-\text{SO}_3\text{H}$) per repeating unit, was determined by a titration method [41]. The membrane was equilibrated in 20ml of 0.05M NaOH for 1h at room temperature, washed with distilled water 30ml. After that, the total volume solution (50ml) was then titrated using phenolphthalein indicator to end-point against 0.05M HCl. The SO_3H group density (mmol/g) calculated as follows [42]:

$$\frac{\text{Amount of } \text{SO}_3\text{H groups} \left(\frac{\text{mmol}}{\text{g}} \right)}{\text{Wt. of sulphonated membrane (g)}} \quad (4)$$

Methanol permeability measurements

A glass diffusion cell [43] composed of two compartments (compartment A) which filled with 2M methanol aqueous solution and (compartment B) which contain distilled water each with an identical volume of 100ml was used to measure the Methanol crossover. The membrane was located vertically between the two compartments (Figure 1) with continuous stirring. Before the test, the membrane was soaked for at least 24h in water to be fully hydrated. The sample solution (500 μL) was withdrawn from the water compartment using a micro-syringe periodically each 25min for 2h and the methanol concentration was then measured using HPLC analysis. All measurements will be carried out

at 25°C. The concentration of methanol in water compartment is related to time by the following equation [44]:

$$C_B(t) = \frac{A \times P}{V_B \times L} C_A(t - t_o) \tag{5}$$

Where P is the methanol permeability, which defined as the product of methanol diffusion coefficient (D) through the membrane and the partition coefficient (K), i.e., (P = DK). C_B is the concentration of methanol in the water compartment (B) at time t. C_A is the initial concentration of methanol in the compartment (A). While A is the membrane working area, L is the membrane thickness, V_B is the volume of water compartment, and t the time lag, which related to the methanol diffusion coefficient (D) as follows: (t_o = L²/ 6D). The methanol permeability (P) obtained from the slope of the linear relationship between the concentration of methanol in the water compartment (C_B) and the time (t) according to the following equation [45]:

$$P = \alpha \frac{V_B}{A} \times \frac{L}{C_A} \tag{6}$$

Where α is the slope of the linear line between C_B versus t.

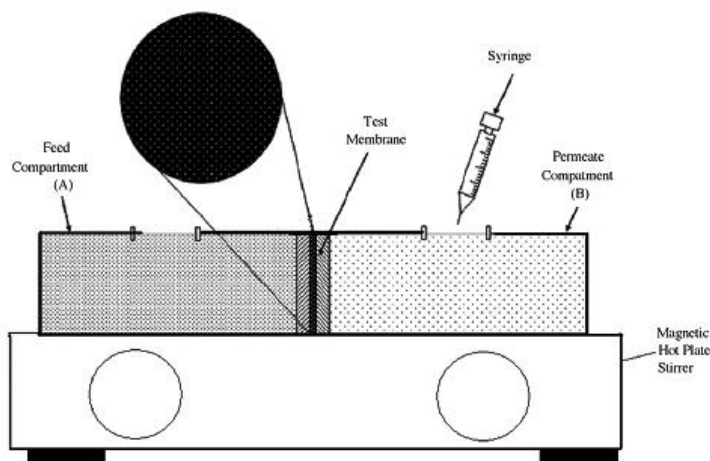


Figure 1: Glass diffusion cell for methanol crossover measurements.

Tensile strength measurement

Tensile strength (TS) is an indication of the resistance of membranes subjected to direct tension. TS is the force required breaking a strip of the sample, which has a specified length and a width of 15mm. LLOYD Instruments LR 10K used for TS measurements. Breaking length (m) equal to TS (kg) length of the strip (m) divided by the strip weight (kg). Where 1kg/15 mm = 3.73 lb/in. Zero-span breaking length ¼ kg breaking load 200,000/ [basis weight/sq in*3]. The sample size is

(1.5-5) cm.

Three measurements were performed at least for each sample, and the mean values reported.

3. RESULTS AND DISCUSSION

3.1. Sulfonation process

Factors affecting sulfonation process such as sodium sulfite concentrations, reaction time, temperature and the solvent ratio explored.

3.1.1. Effect of the sodium sulfite concentration

The effect of variation the SS concentration on the IEC shown in Figure 2. The data showed that there is an increase of IEC with increasing of sodium sulfite concentration from 1 to 5%. Further increase of the SS concentrations leads to a slight decrease in the IEC of sulfonated membranes. This trend could explain by the increase of SS concentration gradient between the liquid phase and the polymer phase. This gradient may lead to increasing the diffusibility of SS into the bulk of the membranes structure through its pores and, as a result, increase the number of attached SS which expressed as IEC increase.

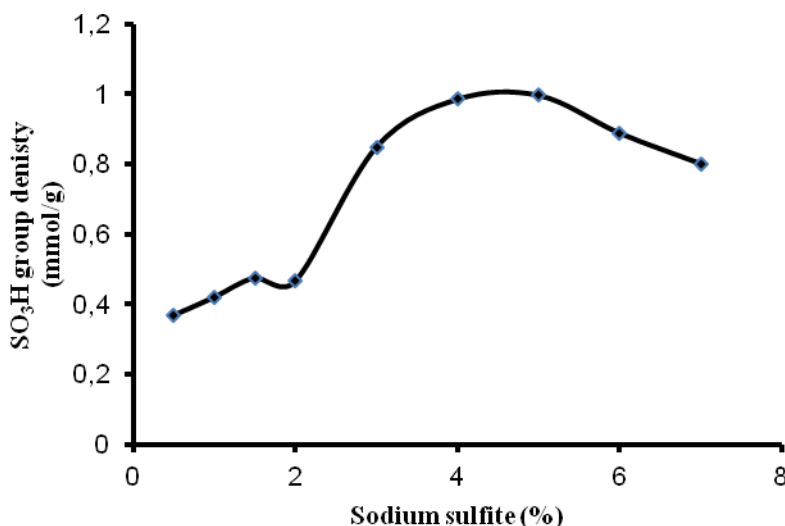


Figure 2. IEC for sulfonated CA membranes at different concentration of sodium sulfite, 30% solvent ratio (30 ml ethanol and 70 ml distilled water), and 2h at 35°C.

3.1.2. Effect of the sulfonation temperature

The effect of variation the sulfonation temperature from 25–65°C on the SCA membranes IEC was shown in Figure 3. Elevating temperature from 25 to 45°C leads to increase the IEC to reach a

maximum value at 45°C; this may be due to increasing the swelling of cellulose matrix and increasing SS solubility. Further elevation of temperature beyond 45°C leads to decrease the IEC of the SCA membranes; this may attribute to the formation of diffusion barrier preventing the sulfonic molecules from reaching to the cellulosic backbone.

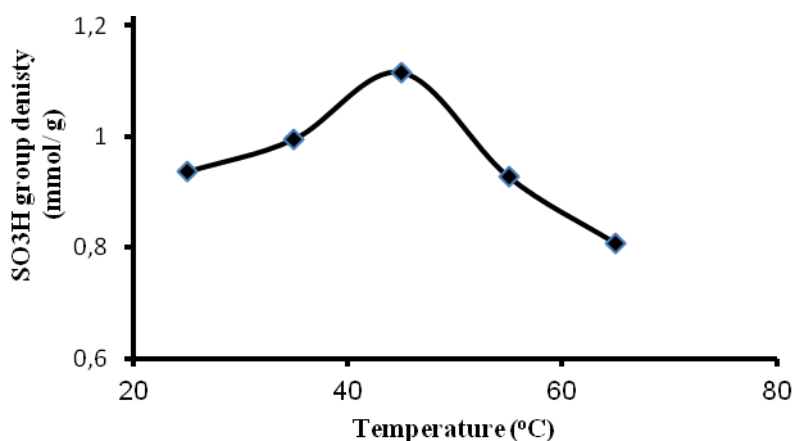


Figure 3. IEC for sulfonated CA membranes at different sulfonation temperatures, 30% solvent ratio (30 ml ethanol and 70 ml distilled water), 5% of sodium sulfite, 2h.

3.1.3. Effect of the sulfonation time

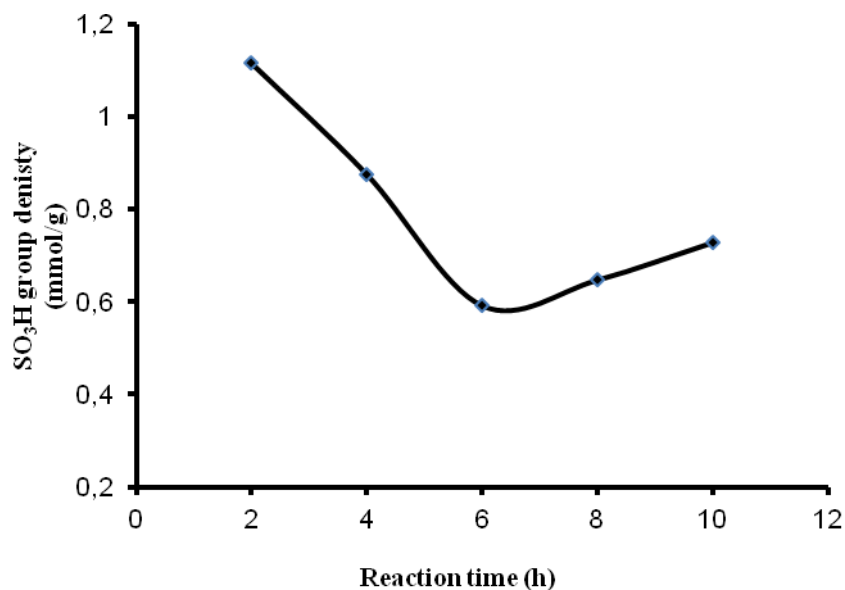


Figure 4. IEC for sulfonated CA membranes at different reaction time, 30% solvent ratio (30 ml ethanol and 70 ml distilled water), 5% of sodium sulfite, 2h, at 45°C.

The effect of variation sulfonation time was shown in Figure 4. The results reveal that

maximum IEC obtained after 2h. Then a further increase in reaction time up to 6h has affected negatively on IEC. These findings may interpret by the hydrophobic diffusion barrier formed during the reaction. Taking into consideration the nature of solvent reaction (Ethanol: Water), which has no swelling ability to the formed sulfonated CA membranes.

3.1.4. Effect of the solvent composition

The effect of variation the solvent composition on the sulfonic group density has been shown in Figure 5. It was evident from the figure that the IEC increase linearly with increase in ethanol percentage to reach a maximum value at 40% ethanol aqueous solution then tends to decrease. This behavior may be explained by increasing the solubility of sulfonic groups and facilitates its diffusion into the activated CA membranes.

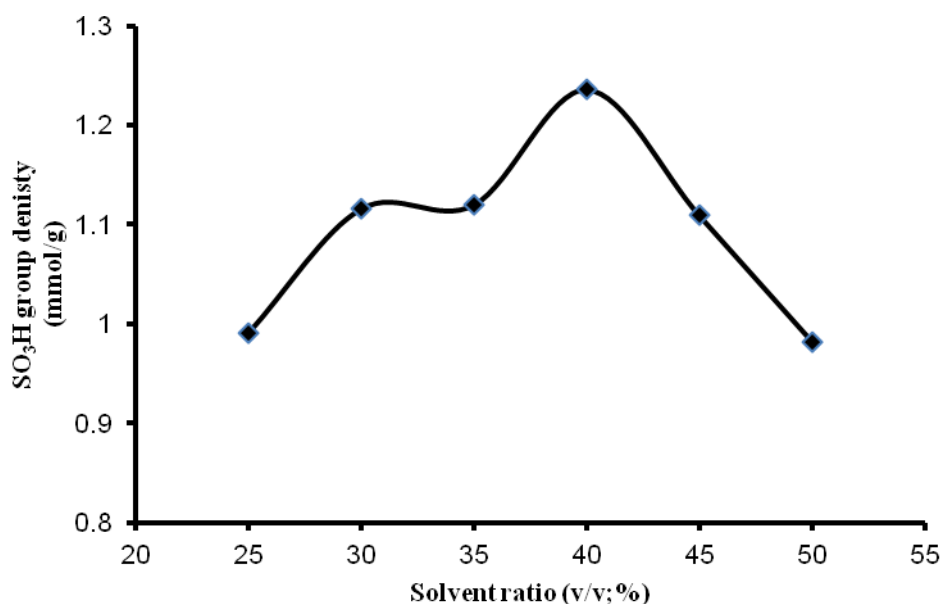


Figure 5. IEC for sulfonated CA membranes at different solvent ratio, 5% of Sodium Sulphite, 2h, at 45°C.

3.2. Membranes characterizations

3.2.1. Water and methanol uptake

The existence of water molecules in sulfonated membranes considerably affected proton and methanol transport through narrow hydrophilic channels surrounded by negatively charged fixed ions, such as a sulfonic acid ($-\text{SO}_3\text{H}$) [47]. Usually, a high degree of sulfonation of polymer membranes leads to high water uptake, poor methanol barrier property, and weak mechanical properties. The data of water and methanol uptakes of sulfonated membranes at different SS concentration, time and solvent ratios presented in Figures 6 (a, b, and c). The obtained data indicated that the sulfonated

membranes had opposite trend in comparison with the native and activated CA membranes despite the hydrophilic nature of the sulphonic groups. This behavior could be explained by the low conversion percentage of epoxy groups into sulfonic ones who confirmed our idea of occurring most of the sulfonation process on the membranes surface leaving the interior completely hydrophobic with unsulfonated epoxy groups. On the other hand, the methanol uptake behavior is almost the same, and this could explain according to the same items due to the similarity of the ionic nature of water and methanol molecules. It should also note that the water uptake of the sulfonated membrane that has an almost same value of IEC as for Nafion[®] 117 (IEC = 0.909 mmol/g [48]) membrane is only 4.016 Wt. %, and is eight times lower than that of Nafion[®] 117. This behavior can explain the fact that the sulfonated membranes are too rigid to be swollen when water molecules penetrate into polymer membrane by hydrophilic interaction with SO_3^- , but the flexible chain of Nafion[®] 117 is freely expanded to form and agglomerate ionic water clusters.

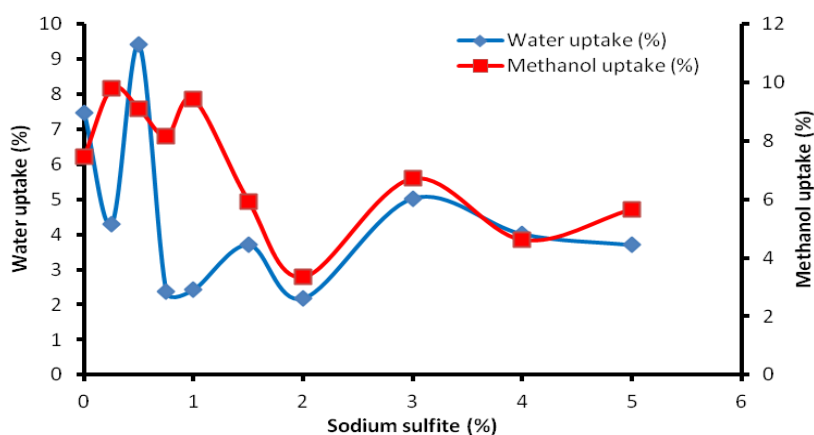


Figure 6a. Water and methanol uptake of sulfonated CA membranes at different concentration of sodium sulfite at 1: 3 molar ratios of CA: ECH respectively, 30% solvent ratio (30 ml ethanol and 70 ml distilled water), 2h and 35°C.

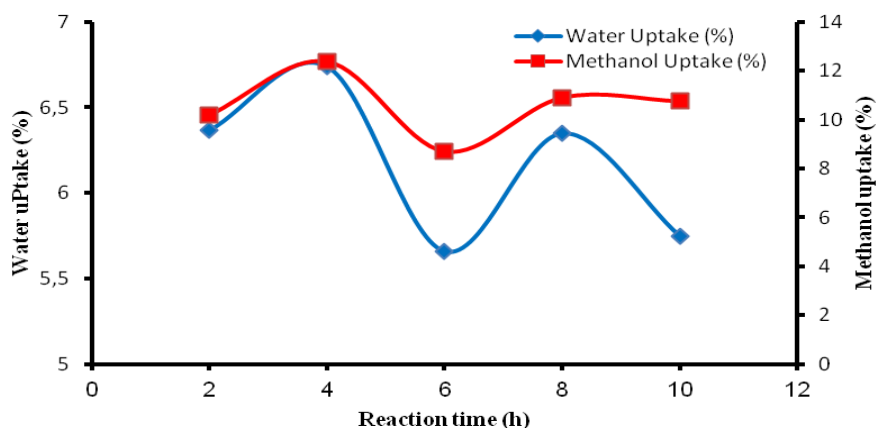


Figure 6b. Water and methanol uptake of sulfonated CA membranes at different reaction time, at 1: 3 molar ratios of CA: ECH respectively, 1% sodium sulfite, 30% solvent ratio (30 ml ethanol and 70 ml distilled water) and 35°C.

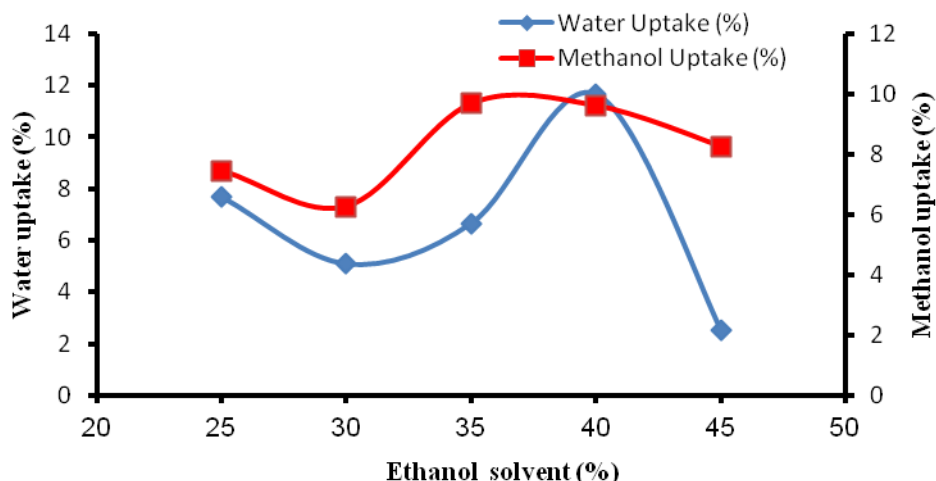


Figure 6c. Water and methanol uptake of sulfonated CA membranes at different solvent ratios of water and ethanol, at 1: 3 molar ratios of CA: ECH respectively, 1% sodium sulfite, 2h, and 35°C.

Figure7 described the relationship between the water uptake and IEC. Usually, a high degree of sulfonation leads to high water absorption, high IEC, poor methanol barrier property, and weak mechanical properties. Meanwhile, the proton conductivity of sulfonated membranes at low IEC values is too little to make them available to the fuel cells. From this point, the fabrication of sulfonated CA membranes can be a desirable approach to limiting severe water uptake even at high IEC and to maintain a proper water sorption level for reasonable proton conduction [49].

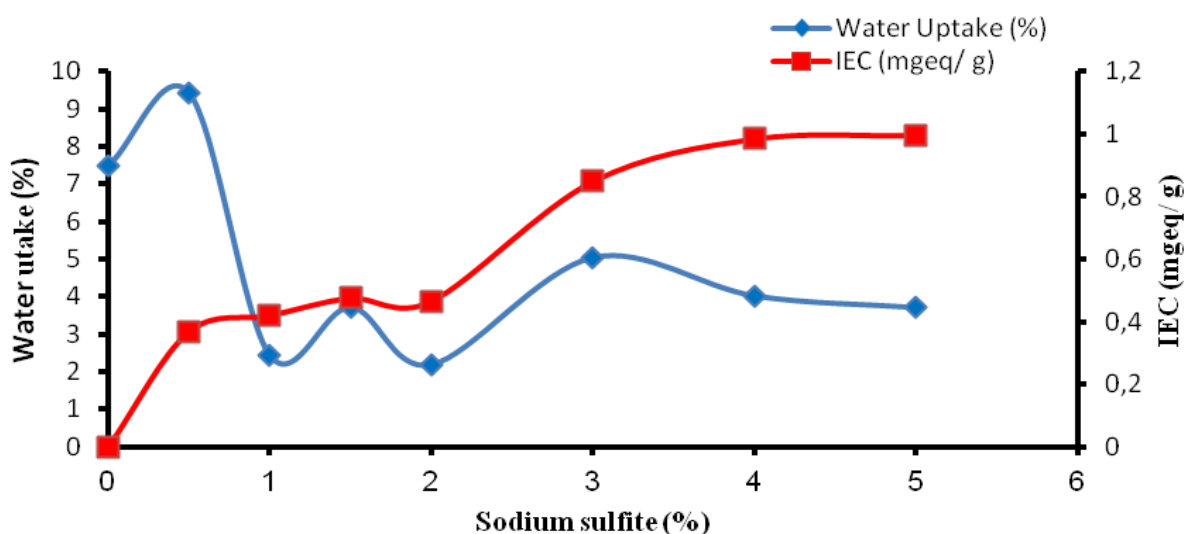


Figure 7. Water uptake and IEC behavior of sulfonated CA membranes at different concentrations of SS, 30% solvent ratio (30 ml ethanol and 70 ml distilled water), 2h at 35°C.

3.2.2. Dimensional changes

The effect of the sulfonation process on the dimensions changes of the SCA membranes after their swelling in water for 24h presented in Tables (1 a and b) for different SS concentration and reaction time. The results showed that the dimensions change significantly changed in comparison with unmodified CA membrane, which confirms that the modification process has an impact on the dimension stability of the modified membranes.

Table 1a. Dimensional changes of sulfonated CA membranes at different concentration of sodium sulfite, for 1.3 molar ratios of CA. ECH respectively, 30% solvent ratio (30 ml ethanol and 70 ml distilled water), 2h and 35°C

Sodium sulfite (%)	Dimension changes in water (%)	Dimension changes in methanol (%)
Original CA membrane	0.0	0.0
ACA membrane	2.5	5
0.25	0.0	0.0
0.5	0.0	0.0
0.75	2.083	0.0
1	0.0	3.448
1.5	2.083	0.0
2	0.0	0.0
3	0.0	0.0
4	3.448	0.0
5	3.45	0.0

Table 1b. Dimensional changes of sulfonated CA membranes at different reaction time, 1% sodium sulfite, for 1.3 molar ratios of CA. ECH respectively, 30% solvent ratio (30 ml ethanol and 70 ml distilled water) and 35°C

Reaction time (h)	Dimension changes in water (%)	Dimension changes in methanol (%)
Original membrane (pure CA)	0.0	0.0
ACA membrane	2.5	5
2	0.0	5.649
4	7.142	7.850
6	0.0	3.448
8	2.127	2.127
10	2.127	5.649

3.2.3. Mechanical characteristics

The tensile properties of original, ACA and SCA membranes were measured, and data recorded in Table 2. The effect of the force on the elongation of the membrane was observed as a positive result while the elongation of the membrane is increased as a result of sulfonation. From results, it was clear

that the sulfonated membranes became more elastic than the un-modified one.

Table 2. Mechanical properties of sulfonated CA membranes at different sodium sulfite concentrations, 30% solvent ratio (30 ml ethanol and 70 ml distilled water), 2h and 35°C

Sodium sulfite (%)	Tensile strength (N)	Elongation (mm)
Original membrane (CA)	15.21	2.645
ACA membrane	45.45	7.75
0.5	37.23	8.507
1	35.13	10.30
1.5	41.45	10.15
2	39.855	9.19
3	49.632	12.10
4	42.572	7.17
5	49.25	12.38
6	35.32	7.33

3.2.4. Optical properties (Color test)

The optical properties of original, ACA and SCA membranes recorded in Table 3 at different SS concentrations. It noticed from the data that there is no significant change in the membrane color surface.

Table 3. Color test for sulfonated CA membranes at different concentration of sodium sulfite, 30% solvent ratio (30 ml ethanol and 70 ml distilled water), 2h and 35°C

Sodium sulfite (%)	L*	a*	b*	ΔE^*
Original membrane (pure CA)	88.04	+0.08	-8.083	49.67
ACA membrane	86.91	+0.07	-8.21	48.88
0.25	87.67	-0.01	-7.85	49.23
0.5	86.61	+0.103	-7.83	48.28
0.75	86.77	+0.043	-7.64	48.41
1	87.287	+0.077	-7.657	48.82
1.5	87.377	-0.027	-7.797	48.99
2	87.23	+0.05	-7.64	48.77
3	86.52	+0.037	-7.823	48.33
4	87.36	-0.027	-7.673	48.887
5	87.747	-0.307	-7.73	49.24
6	87.53	-0.247	-7.52	48.67

3.2.5. Surface roughness test

Table 4 represent the surface roughness parameters for the original, ACA and SCA membranes, from the results, obtained it was clear that the parameters for all membranes nearly are the same which

means that the modification process has no change on the surface CA membranes.

Table 4. Surface Roughness parameters for sulfonated CA membranes at different concentration of sodium sulfite, 30% solvent ratio (30 ml ethanol and 70 ml distilled water), 2h and 35°C

Sodium sulfite (%)	Ra (μm) for the upper surface	Ra (μm) for the lower surface
Original CA membrane	0.05	0.08
ACA membrane	0.066	0.064
0.5	0.04	0.046
1	0.056	0.052
1.5	0.054	0.06
2	0.034	0.051
3	0.051	0.046
4	0.046	0.061
5	0.068	0.096
6	0.058	0.078

3.2.6. Thermal oxidation stability

Figure 8 showed that the SCA membranes are exhibit highly thermal oxidative stable under high temperature (up to 80°C) after 48h. Also, the %weight loss of membranes ranged from (8-15%) with increasing SS concentration from (0.25 to 6%) while the ACA membrane lost about 5% from the initial weight. These results may attribute to the nature of SCA due to the presence of SO³⁻ groups which responsible for the weight loss.

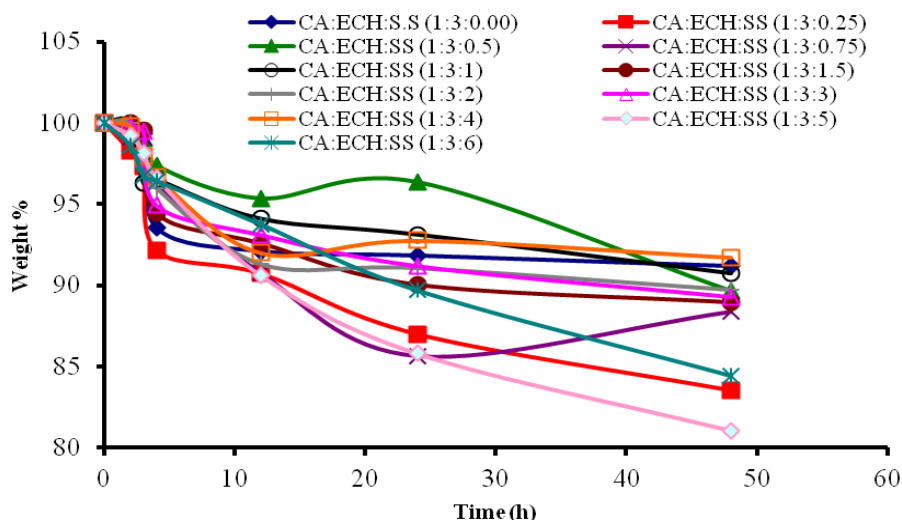


Figure 8. Thermal oxidation stability of original, ACA, and SCA membranes with different concentrations of SS.

3.2.7. FTIR spectrophotometric analysis

FTIR spectra for original, ACA, and SCA membranes illustrate the evidence of sulphonation processes as shown in Figure 9. The results indicated that the opening of the epoxy rings through sulfonation process have been occurred through the appearance of three characteristic bands for the sulfonic group at 1051, and 599 cm^{-1} . The remaining characteristic bands for epoxy rings indicate incomplete sulfonation reaction.

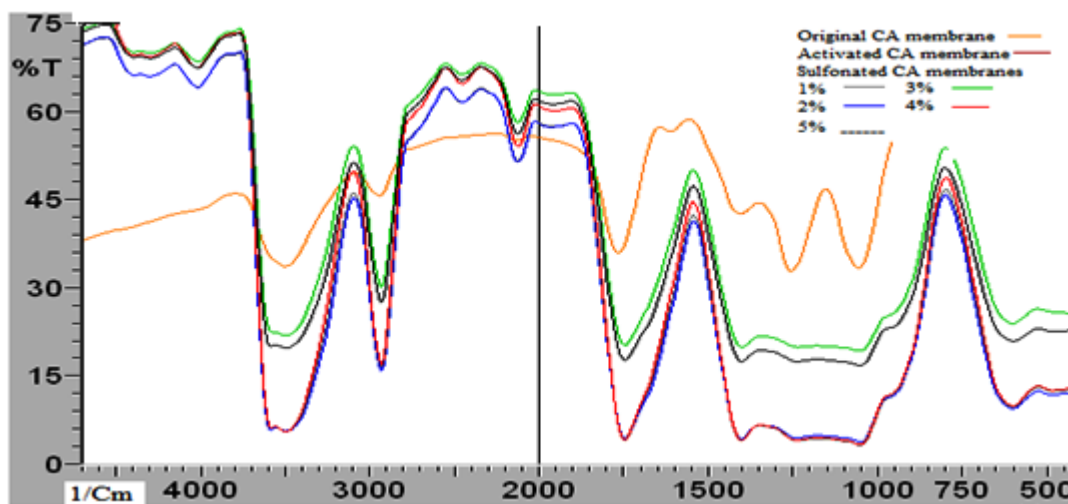


Figure 9. FTIR spectra of (1) original CA membrane, (2) ACA membranes, and ((3) 1%, (4) 2%, (5) 3%, (6) 4%, and (7) 5% sulfonated CA membranes).

3.2.8. Thermal gravimetric analysis (TGA)

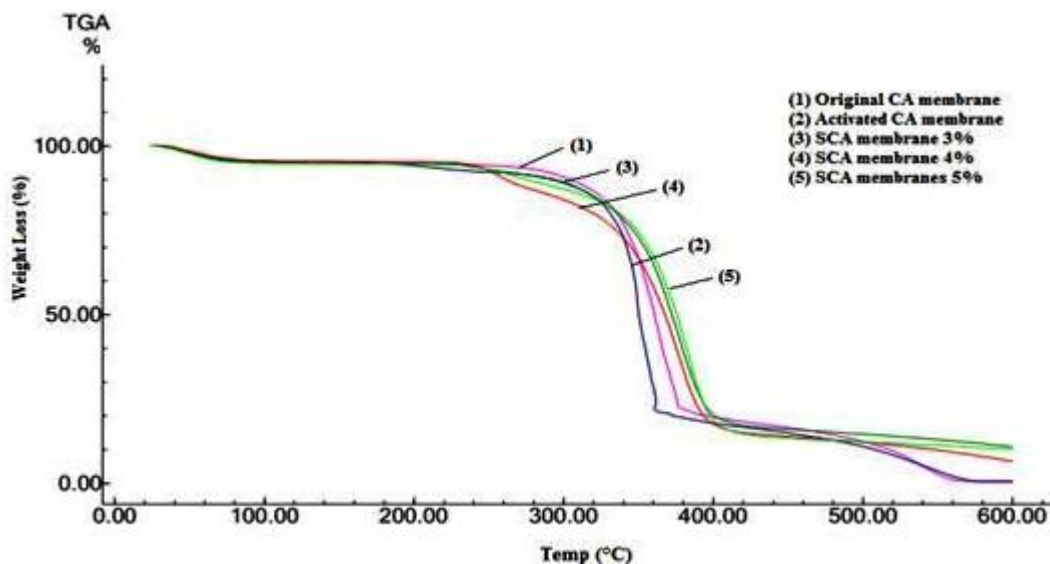


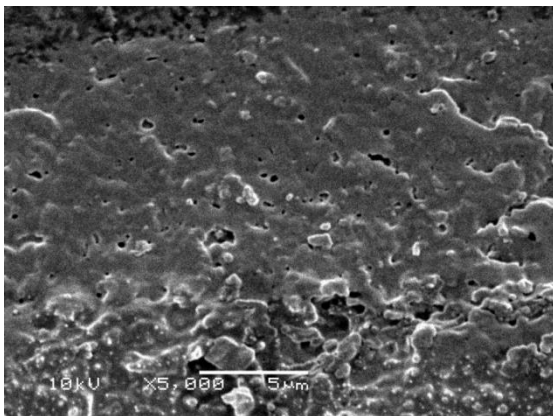
Figure 10. TGA thermograph of original, ACA, and SCA membranes at different SS concentration.

The obtained results from TGA analysis is shown in Table 5 and Figure 10. It was clear that SCA membranes are thermally stable than the original and ACA membranes as $T_{50} = 375.72^{\circ}\text{C}$ which mean that sulfonation process improved the membrane hydrophilicity to a great extent by introducing sulfonic groups.

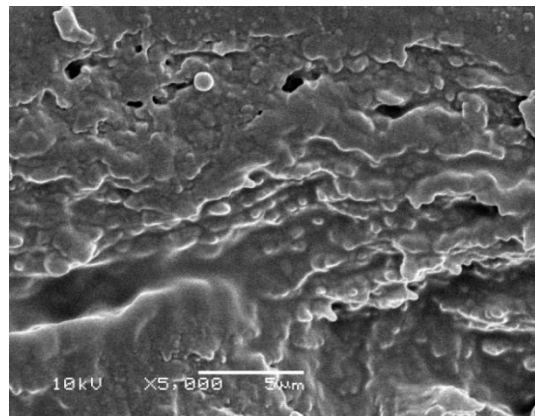
Table 5. TGA analysis for original activated and sulfonated CA membranes

Membrane with molar ratio	T_{50}	Weight loss (%) at ambient temperature (0-150°C)
Original CA membrane	360.83	4.611
ACA (1: 3)	350.23	4.75
SCA (1: 3: 3)	374.84	5.15
SCA (1: 3: 4)	367.86	3.09
SCA (1: 3: 5)	375.72	3.01

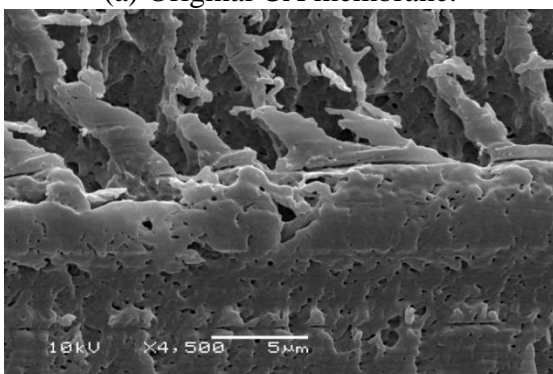
3.2.9. Morphological characterization (SEM)



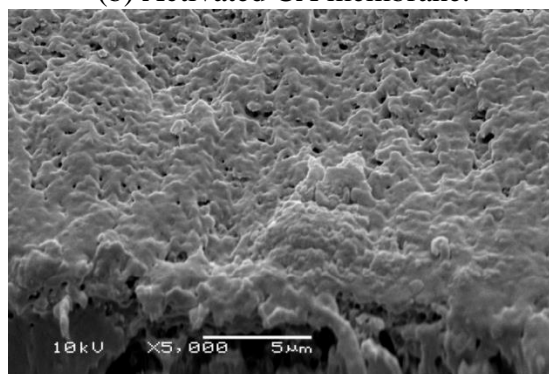
(a) Original CA membrane.



(b) Activated CA membrane.



(c) SCA membrane (1% SS).



(d) SCA membrane (1.5% SS).

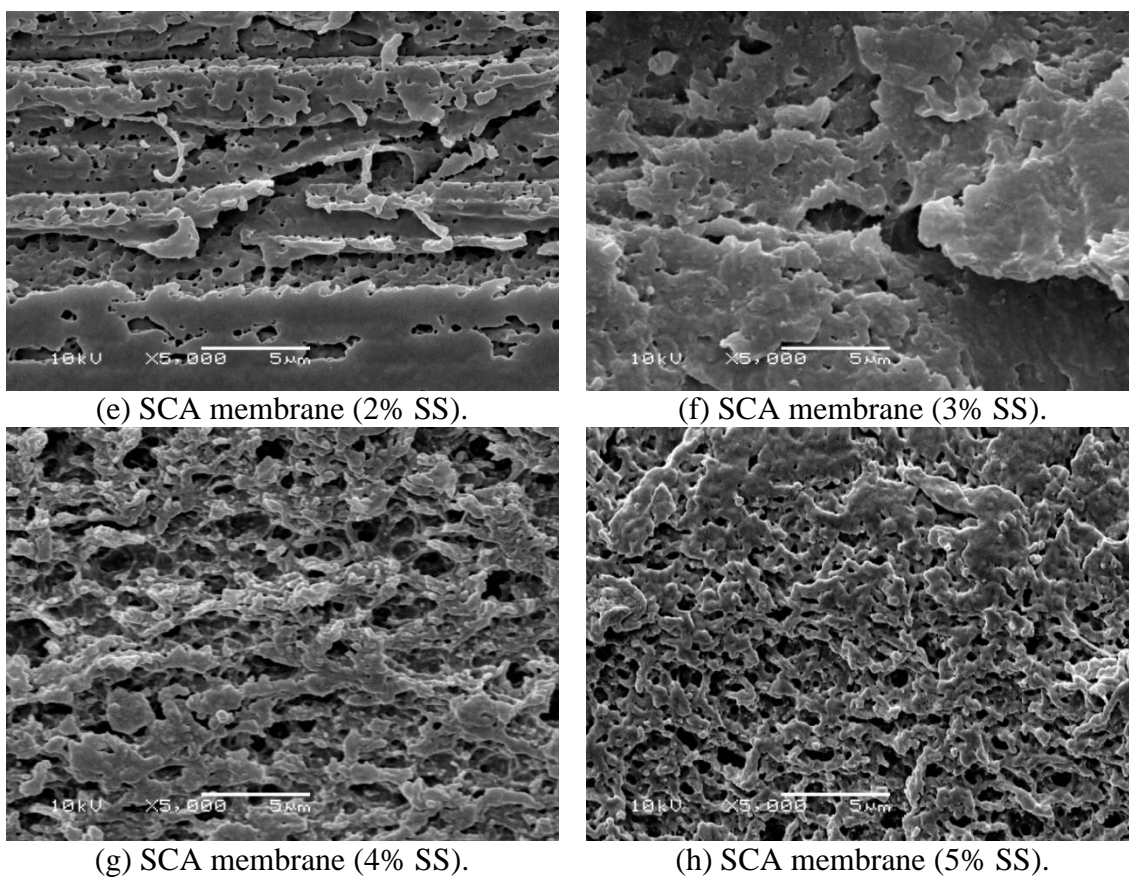


Figure 11: SEM Micrograph of original CA, ACA and SCA membranes at different SS concentrations.

The morphological change of original, ACA and SCA membranes with different concentrations of SS represented in Figure 11. It was clear from the figures that the morphological structure of the sulfonated CA membranes differed than the original CA and the activated CA membranes, i.e., increasing the porosity and roughness property. Thus, changes the structure as a result of the sulfonation process.

3.2.10. X-ray diffraction analysis (XRD)

Figure 12 showed the wide-angle X-ray diffractograms of original CA, activated CA and sulfonated CA membranes. It was clear that a broad diffraction feature appeared at $2\theta = 21.295\text{--}22.6^\circ$, $22.18\text{--}22.83^\circ$, and $22.385\text{--}24.41^\circ$ for the original, the activated and the sulfonated CA membranes respectively, while the interlayer distances were 0.424, 0.4, 0.397nm for original, activated and (3%) sulfonated CA membranes respectively. The slight difference in the data indicates that the sulfonation had no significant effect on the membrane structure [47].

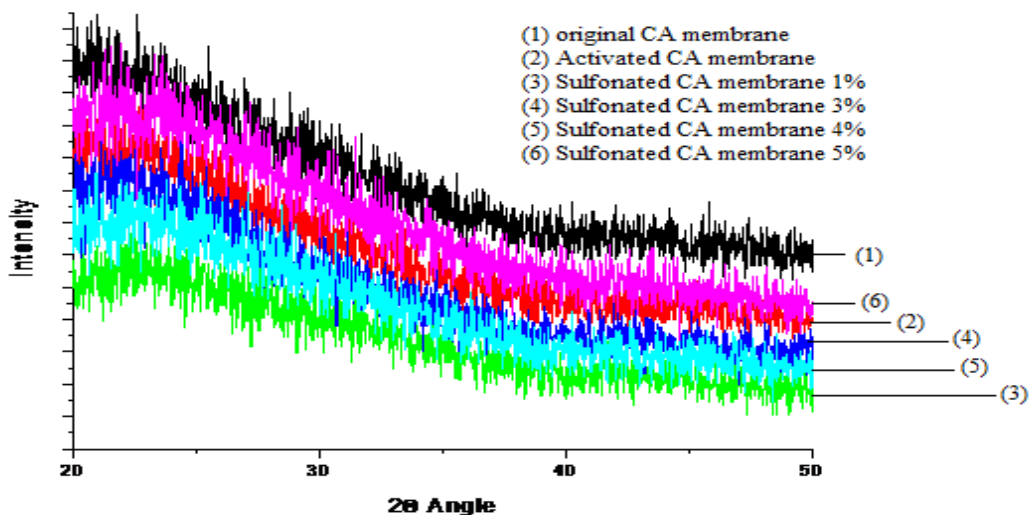


Figure 12. XRD of original CA, ACA and SCA membranes.

3.2.11. Methanol permeability measurement

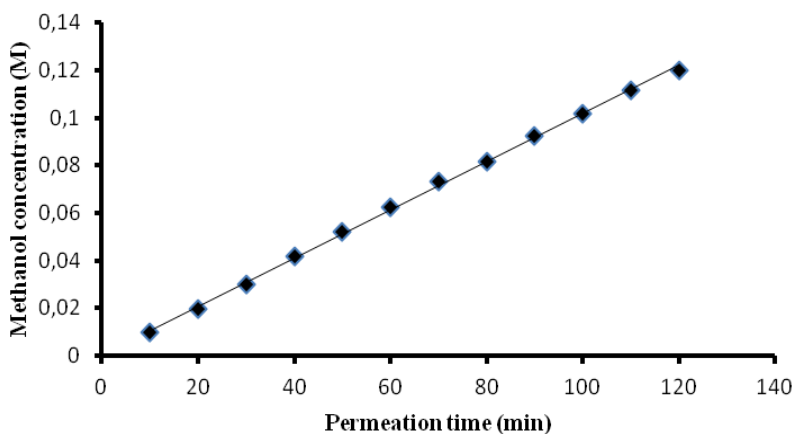


Figure 13. Methanol concentration as a function of permeation time for Nafion® 117 membrane.

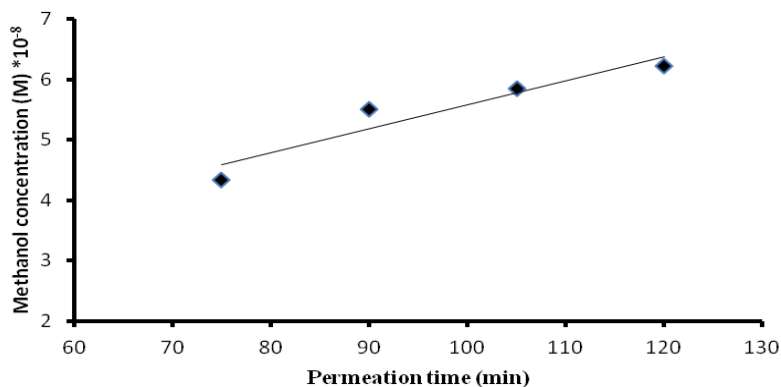


Figure 14. Methanol concentration as a function of permeation time for the sulfonated membrane.

Figures 13 and 14 represented the change in methanol concentration versus the permeation time. By calculating the slope of the line it was clear that the methanol permeability of the sulfonated membrane is $1.729 \times 10^{17} \text{ cm}^2/\text{S}$ compared to $1.14 \times 10^9 \text{ cm}^2/\text{S}$ for Nafion[®] 117 which indicated that the sulfonation process was effective in decreasing the methanol crossover to a great extent [50].

4. CONCLUSION

Novel SCA membranes are easy to prepare and much less expensive than the commercial Nafion[®] membranes. It was synthesized for the first time and characterized by FT-IR, SEM, TGA, and XRD. The results obtained from FTIR proved that the sulfonate groups were indeed quantitatively introduced into the surface of CA membrane as expected. While, TGA and XRD measurements proved that the prepared membranes have an excellent thermal properties and flexibility. SEM micrographs showed that sulfonic acid groups uniformly distributed within the polymer matrix. The IEC, liquid uptake, dimensional stability, and methanol permeability have compared with those of the original CA membranes and Nafion[®]117 membranes. Attractive properties were found such as; enhanced excellent thermal and mechanical stabilities, lower liquid uptake in water and methanol solution. The methanol permeability of the SCA membranes under the conditions of (1:3 molar ratio of CA: ECH respectively, 5% SS, 2h, 45°C, and 40% methanol ratio) was little as $1.729 \times 10^{17} \text{ cm}^2/\text{S}$ compared with $1.14 \times 10^9 \text{ cm}^2/\text{S}$ of Nafion[®]117. Therefore, the SCA poly PEMs can be candidates for DMFCs applications.

References

1. S. Surampudi, S.R. Narayanan, E. Vamos, H. Frank, G. Halpert, A. LaConti, J. Kosek, G. Prakash, G.A. Olah, *J Power Sources* 47 (1994) 377.
2. M. Winter, R.J. Brodd, *Chem. Rev.* 104 (2004) 4245–4269.
3. F. Lufrano, V. Baglio, P. Staiti, V. Antonucci, A.S. Arico, *J Power Sources* 243 (2013) 519-534.
4. N.A. Hampson, M. J. Willars, B. D. McNicol, *J Power Sources* 4 (1979) 191.
5. X. Ren, M.S. Wilson, S. Gottesfeld, *J Electrochem. Soc.* 143 (1996) L12.
6. Y.F. Huang, L.C. Chuang, A.M. Kannan, C.W. Lin, *J Power Sources* 186 (2009) 22.
7. I. Honma, H. Nakajima, O. Nishikawa, T. Sugimoto, S. Nomura, *Solid-State Ionics* 162/163 (2003) 237–245.
8. C. Zhao, H. Lin, H. Na, *Int. J Hydrogen Energy* 35 (2010) 2176–2182.
9. M.A. Hickner, H. Ghassemi, Y.S. Kim, B.R. Einsla, J.E. McGrath, *Chem. Rev.* 104 (2004) 4587-4611.
10. A. Chandan, M. Hattenberger, A. El-Kharouf, S.F. Du, A. Dhir, V. Self, B.G. Pollet, A. Ingram, W. Bujalski, *J Power Sources* 231 (2013) 264-278.
11. W.C. Choi, J.D. Kim, S.I. Woo, *J Power Sources* 96 (2001) 411.
12. A. Küver, W. Vielstich, *J Power Sources* 74 (1998) 211.
13. W.H.J. Hogarth, J.C. Diniz da Costa, G.Q. Lu, *J Power Sources* 142 (2005) 223.
14. P. Krishnan, J.S. Park, C.S. Kim, *Eur. Polym. J* 43 (2007) 4019–4027.
15. P. Dimitrova, *Solid State Ionics.*, 150 (2002) 115–22.
16. L. Wang, Y.Z. Meng, S.J. Wang, X.Y. Shang, L. Li, A.S. Hay, *Macromolecules.*, 37(2004) 3151–3158.

17. D. Mecerreyes, H. Grande, O. Miguel, E. Ochoteco, R. Marcilla, I. Cantero, *Chem Mater.*, 16 (2004) 604–607.
18. L. Wang, Y.Z. Meng, S.J. Wang, X.H. Li, M. Xiao, *J Polym Sci., Part A: Polym. Chem.* 43 (2005) 6411–6418.
19. P. Xing, G.P. Robertson, M.D. Guiver, S.D. Mikhailenko, S. Kaliaguine, *Macromolecules.*, 37 (2004) 7960–7967.
20. P. Xing, G.P. Robertson, M.D. Guiver, S.D. Mikhailenko, S. Kaliaguine, *Polymer.*, 46 (2005) 3257–3263.
21. F. Lufrano, I. Gatto, P. Staiti, V. Antonucci, E. Passalacqua, *Solid State Ionics.*, 145 (2001) 47–51.
22. K. Okamoto, Y. Yin, O. Yamada, M.N. Islam, T. Honda, T. Mishima, Y. Suto, K. Tanaka, H. Kita, *J Membr Sci.*, 258 (2005) 115–122.
23. Y. Shang, X.F. Xie, H. Jin, J.W. Guo, Y.W. Wang, S.G. Feng, S.B. Wang, J.M. Xu, *Eur Polym J.*, 42 (2006) 2987–2993.
24. T. Watari, J.H. Fang, K. Tanaka, H. Kita, K. Okamoto, T. Hirano, *J Membr Sci.*, 230 (2004) 111–120.
25. Y.S. Choi, T.K. Kim, E.A. Kim, S.H. Joo, C. Pak, Y.H. Lee, *Advanced Materials* 20 (2008) 2341–2344.
26. C. Zhang, X.X. Guo, J.H. Fang, H.J. Xu, M.Q. Yuan, B.W. Chen, *J Power Sources.*, 170 (2007) 42.
27. J.A. Kerres, *J Membr Sci.*, 185 (2001) 3–27.
28. D.J. Jones, J.J. Roziere, *J Membr Sci.*, 185 (2001) 41–58.
29. N. Carretta, V. Tricoli, F. Picchioni, *J Membr Sci.*, 166 (2000) 189–197.
30. G.Q. Wang, X.L. Zhu, S.H. Zhang, Y.F. Liang, X.G. Jian, *Acta Polym Sin.*, 2 (2006) 209–212.
31. M. Gil, X.L. Ji, X.F. Li, H. Na, J.E. Hampsey, Y.F. Lu, *J Membr Sci.*, 234 (2004) 75–81.
32. P.X. Xing, G.P. Robertson, M.D. Guiver, S.D. Mikhailenko, K. Wang, S. Kaliaguine, *J Membr Sci.*, 229 (2004) 95–106.
33. S. Swier, Y.S. Chun, J. Gasa, M.T. Shaw, R.A. Weiss, *Polym Eng Sci.*, 45 (2005) 1081–1091.
34. Y.S. Kim, M.A. Hickner, L.M. Dong, B.S. Pivovar, J.E. McGrath, *J Membr Sci.*, 243 (2004) 317.
35. D. Poppe, H. Frey, K.D. Kreuer, A. Heinzl, R. Mulhaupt, *Macromolecules.*, 35 (2002) 7936–7941.
36. B.J. Liu, G.P. Robertson, M.D. Guiver, Y.M. Sun, Y.L. Liu, J.Y. Lai, S. Mikhailenko, S. Kaliaguine, *J Polym Sci. Part B: Polym Phys.*, 44 (2006) 2299.
37. S. Mohy Eldin, M. H. Abd Elmageed, A. M. Omer, T. M. Tamer, M. E. Yossuf, R. E. Khalifa., *Int J Electrochem Sci.*, (2016).
38. M. Theodor, N. Raluco, and I.P. Valentin, *bioresources.*, 3(4) (2008) 1371–1376.
39. C. Yang, W. Chien, and Y. J. Li, *International Journal of Hydrogen Energy.*, 36 (2010) 3407–3415.
40. C. Tseng, Y. Ye, K. Kao, J. Joseph, W. Shen, J. Rick, and B. Hwang, *International Journal of Hydrogen Energy.*, 36 (2011) 11936–11945.
41. A. Panchenko, H. Dilger, E. Möller, T. Sixt, E. Roduner. *J Power Sources.*, 30 (2004) 127–325.
42. P. Xing, G.P. Robertson, M.D. Guiver, S.D. Mikhailenko, K. Wang, S. Kaliaguine, *Journal of Membrane Science.*, 229 (2004) 95–106.
43. M.S. Mohy Eldin, E.A. Soliman, E.A. Hassan, M.A. Abu-Saied, *Journal of Applied Polymer Science.*, 111 (2009) 2647–2656.
44. V. Tricoli. *J. Electrochem. Soc.* 145 (1998) 3798–3801.
45. M.M. Nasef, N.A. Zubir, A.F. Ismail, M. Khayet, K.Z.M. Dahlan, H. Saidi, R. Rohani, T.I.S. Ngaha, N.A. Sulaiman. *J. Membr. Sci.* 268 (2006) 96–108.
46. N. I. El-Awady, M. M. El-Awady, M. S. Mohy Eldin, *Egy J Polym Sci Technol.*, 3 (1999) 25–41.
47. D. Xing, G. He, Z. Hou, P. Ming, S. Song, *International Journal of Hydrogen Energy.* 36 (2011) 2177–2183.

48. T.A. Zawodzinski, C. Derouin, S. Radzinski, R.J. Sherman, V.T. Smith, T.E. Springer, S. Gottesfeld, *Journal of Electrochemical Society*. 140 (1993)1041-1047.
49. V.S. Rangasamy, S. Thayumanasundaram, N.D. Greef, J.W. Seo, J.P. Locquet, *Solid State Ionics.*, 216 (2012) 83–89.
50. A. B. A. Amine, Preparation of Polyelectrolyte Membranes and Electrodes for Direct Methanol Fuel Cells, MSc thesis, Faculty of Science AL-Azhar University, Egypt, 2007.

© 2016 The Authors. Published by ESG (www.electrochemsci.org). This article is an open access article distributed under the terms and conditions of the Creative Commons Attribution license (<http://creativecommons.org/licenses/by/4.0/>).